IEEE Photonics Journal
An IEEE Photonics Society Publication

Open Access

Quasi-Distributed Dual-Parameter Optical Fiber Sensor Based on Cascaded Microfiber Fabry–Perot Interferometers

Volume 10, Number 2, April 2018

Yang Xiang
Yiyang Luo
Yanpeng Li
Yue Li
Zhijun Yan
Deming Liu
Qinzhen Sun

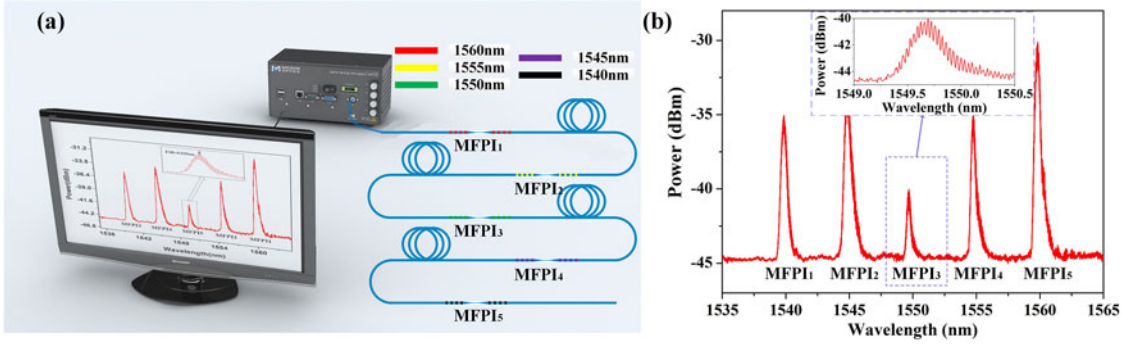

DOI: 10.1109/JPHOT.2018.2817573
1943-0655

Quasi-Distributed Dual-Parameter Optical Fiber Sensor Based on Cascaded Microfiber Fabry–Perot Interferometers

Yang Xiang, Yiyang Luo, Yanpeng Li, Yue Li, Zhijun Yan, Deming Liu, and Qinzhen Sun

School of Optical and Electronic Information, National Engineering Laboratory for Next Generation Internet Access System, Huazhong University of Science and Technology, Wuhan 430074, China

DOI:10.1109/JPHOT.2018.2817573

Manuscript received February 2, 2018; accepted March 15, 2018. Date of current version April 6, 2018. This work was supported in part by the National Natural Science Foundation of China under Grants 61275004 and 61775072, in part by the subproject of the major program of the National Natural Science Foundation of China under Grants 61290315 and 61290311, in part by the Wuhan Morning Light Plan of Youth Science and Technology (2017050304010280), and in part by the Fundamental Research Funds for the Central Universities (HUST: 2015ZDTD013). Corresponding author: Qinzhen Sun (e-mail: qzsun@mail.hust.edu.cn).

Abstract: We propose and demonstrate a quasi-distributed fiber sensor based on cascaded microfiber Fabry–Perot interferometers (MFPIs) for simultaneous refractive index (RI) and temperature measurement. By employing MFPI that is fabricated by taper-drawing the center of a uniform fiber Bragg grating on standard fiber into a section of microfiber, dual-parameters including RI and temperature can be detected through demodulating envelop and resonant wavelength of the reflection spectrum of the MFPI. Then, wavelength-division-multiplexing is applied to realize quasi-distributed dual-parameter sensing by using cascaded MFPIs with different Bragg wavelengths. A prototype sensor system with five cascaded MFPIs is constructed to experimentally demonstrate the sensing performance. The quasi-distributed dual-parameter sensing system has great significance on monitoring gradient parameter-variations in chemical and biological sensing applications.

Index Terms: Optical sensors, remote sensing, temperature measurement, refractive index, and microstructure.

1. Introduction

In recent years, fiber-based sensors have been intensively investigated for measurement of chemical, physical and biomedical parameters owing to their distinctive merits, such as compact structure, ease of fabrication, excellent real-time monitoring capability and low cost [1]–[4]. Especially, to well expose the physic properties of materials, refractive index (RI) and temperature measurements are significant and irreplaceable.

So far, many fiber-based structures have been proposed for RI or temperature monitor. For instances, some structures were proposed for RI sensor including tapered fiber probe [5], singlemode-multimode-singlemode fiber structure [6] and inline Mach-Zehnder-interferometer [7]. There were also several methods liking fiber Sagnac interferometer [8], Fabry-Perot interferometer [9] and side-polished single-mode fiber covered with the polymer planar waveguide [10], constructed for temperature sensor. However, only single parameter (temperature or RI) can be measured by these

sensors. Recently, for higher-efficient environment sensing and eliminating the cross affection of temperature to RI, dual-parameter measurement was investigated. Owing to the higher temperature sensitivity and simpler structure, fiber Bragg grating (FBG) is an important candidate. A sensing head consisting of a core-offset MZI and FBG, was constructed by Yao et al to realize the temperature and RI measurement based on the modulation of interferometer fringe as well as Bragg wavelength [11]. And an Up-Fusion-Bitaper pair is combined with an embedded FBG for dual-parameter sensing through fiber model interference [12]. Specially, converted FBGs such as FBG-probe, FBG-microfiber structure, sampled FBG, were also introduced to realize the measurement of temperature and RI [13], [14]. Except for FBG, the long-period fiber grating [15], [16] and Sagnac loop [17] can also achieve the dual-parameter sensing. Moreover, some other technologies such as etched micro-wires [18], tapered micro-wires [19] and silica micro-wires [20] are helpful to improve the dual-parameter performance. However, all the above works have not been involved in a quasi-distributed sensing which is important to monitor the real-time change of the temperature and RI distribution gradient of gas, liquid and so on.

Microfiber has attracted increasing research interest due to the well-known low-loss characteristic as silica wave guides [21]. Besides, it has been demonstrated in different applications such as add-drop filter [22], lasing systems [23], [24], nonlinear optics [25] and fiber sensors [26]. Owing to the small diameter and large evanescent field, the microfiber devices are sensitive to changes of the external environment, particularly the RI of the ambient medium. In these years, a lot of novel structures based on microfiber have been explored to realize the simultaneous measurement of RI and temperature [27]–[32]. Especially, in our previous works [33], we have proposed and demonstrated a dual-parameter measurement scheme combining microfiber and FBGs. Its inline structure and low transmission loss can help constituting a quasi-distributed sensor system.

In this paper, a quasi-distributed fiber sensor system is proposed and realized for simultaneous measurement of RI and temperature. The sensor elements, composed of a piece of microfiber sandwiched between two uniform FBGs to constitute a microfiber Fabry-Perot interferometer (MFPI), are deployed along the sensing optical fiber. Due to the different formation mechanisms between the fringes and the envelope on the spectrum of MFPI, they are changing in different functional relationships with the variation of temperature and RI. Furthermore, a sensing matrix will be built to describe the complex relationship between temperature, RI and fringes, envelop. As a result, the dual-parameter can be demodulated from the sensing matrix. Further, by introducing Wavelength-Division-Multiplexing (WDM) mechanism, the variation and distribution of the external environment parameters can be monitored based on the analysis of the spectrum shift.

2. Schematic Diagram and Properties of the Sensor System

Fig. 1(a) illustrates the schematic diagram of the MFPI sensor element, which consists of two identical FBGs and a length of microfiber. Different from traditional Fabry-Perot fiber sensor, the FBG-microfiber-FBG structure is more susceptible to RI by virtue of its large evanescent field which contacts the signal light closer with external conditions. Simultaneously, two pieces of FBGs can be sensitive to ambient temperature due to thermo-optic effect. Further, based on the MFPIs constructed by FBGs of different Bragg wavelengths, WDM technique is introduced to realize the function of positioning and build a quasi-distributed dual-parameter sensing system as shown in Fig. 1(b).

For the fabrication of the quasi-distributed sensing structure, we firstly introduce the online inscribing technology to get a string of FBGs with different Bragg wavelengths along a standard fiber. Then, a piece of microfiber is conveniently fabricated by applying the flame brushing technique at the center part of FBG. Specifically, the diameter of microfiber can be roughly adjusted by controlling the drawing rate and the length of heating region while the length of microfiber is determined by the drawing distance. After been drawn to small diameter at such high temperature, the heating part of FBG structure will be erased completely, making the tapered FBG indifferent to normal

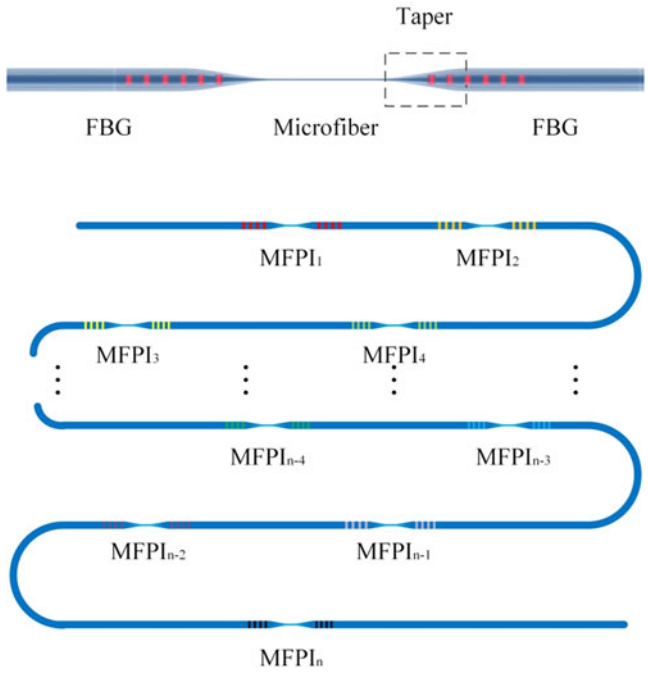

Fig. 1. (a) Schematic illustration of MFPI. (b) Schematic diagram of the quasi-distributed dual-parameter optical fiber sensor system.

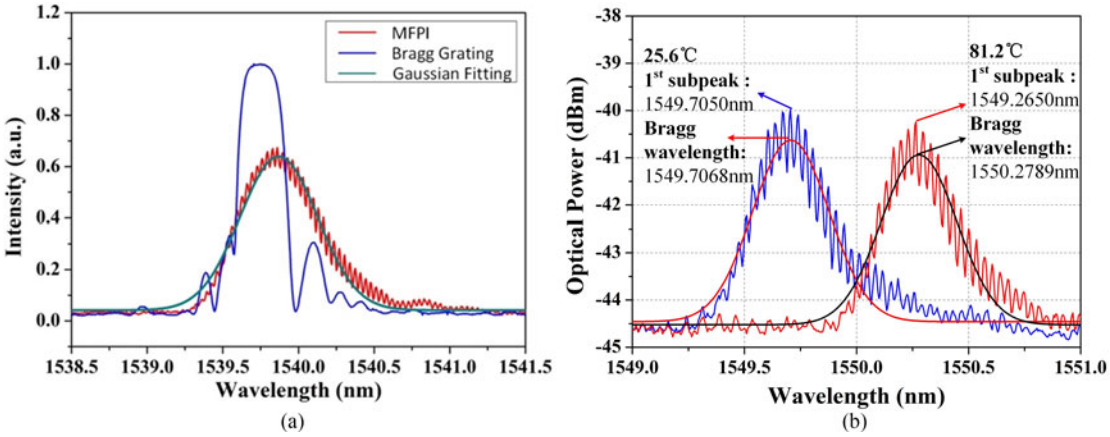

Fig. 2. (a) Typical reflection spectrum of Bragg grating, MFPI and Gaussian Fitting of MFPI. (b) The reflection spectra and Gaussian Fittings of a MFPI sample at 25.6 °C (blue line) and 81.2 °C (red line).

single-mode-fiber and thus, the microfiber part can be regarded as a low loss resonant cavity. In this way, MFPI with cascaded FBG-microfiber-FBG structure is constituted. It should be noted that flame heating might cause some deformation to FBG, and there may be residual grating structures on the tapers, which are slightly stretched, i.e., chirped. As a result, FBG in MFPI will have stronger reflection at the long wavelength side of its reflection band compared to a uniform FBG. Besides, the 3-dB band-width broadens and spectrum turns into intensive modulation from a smooth curve as depicted in Fig. 2. Then, the above tapering operation is conducted to each FBG of different Bragg wavelengths and the quasi-distributed sensing fiber, i.e., the cascaded MFPIs with WDM, can be achieved.

The corresponding sensitivities of Bragg wavelength and resonant peak to temperature and RI can be expressed as [33]–[36]:

$$\frac{\partial \lambda_m}{\partial n_{am}} = \frac{4\pi l}{m2\pi - \varphi_0} \times \frac{\partial n_{eff}}{\partial n_{am}} \tag{1}$$

$$\frac{\partial \lambda_B}{\partial n_{am}} = 0 \tag{2}$$

$$\frac{\partial \lambda_B}{\partial T} = \lambda_B (\alpha + \xi) \tag{3}$$

$$\frac{d\lambda_m}{dT} = (\alpha + \xi) \frac{\lambda_m}{n_{eff}} \frac{\partial n_{eff}}{\partial n_{core}} + (\xi_{am} + \alpha) \frac{\lambda_m}{n_{eff}} \frac{\partial n_{eff}}{\partial n_{am}} \tag{4}$$

where m represents the order of resonant peak; λ_m is the original wavelength of the m-th order resonant peak; n_{am} is the ambient RI; l is the length of microfiber; φ_0 is the initial phase of the incident light; $n_{eff} = \lambda_0 \beta'/(2\pi)$ is effective refractive index of microfiber (β' is the propagation constant in the microfiber); λ_B is the Bragg wavelength of the MFPI; α and ξ are the thermo-optic coefficient and thermal expansion coefficient of the optical fiber, respectively; n_{core} is the RI of fiber core; ξ_{am} is the thermo-optic coefficients of ambient media. In consideration of the fact that two parts of FBGs are single-mode-fibers with guide-mode only in fiber core and free from ambient medium, we can affirm that the ambient RI has no impact on Bragg wavelength.

Knowing that for specific MFPI, the parameters on the right of (1)–(4) are all constant, we conclude that there are linear relationships between $\Delta\lambda_m$, $\Delta\lambda_B$ and temperature, RI, separately. By tracking the Bragg wavelength and certain resonant peak of MFPI, it is able to demodulate temperature and RI variations simultaneously. In view of the Bragg wavelength independent of RI, the sensing function can be written as:

$$\begin{bmatrix} \Delta\lambda_m \\ \Delta\lambda_B \end{bmatrix} = \begin{bmatrix} A & B \\ 0 & D \end{bmatrix} \begin{bmatrix} \Delta RI \\ \Delta T \end{bmatrix} \tag{5}$$

where A and B respectively represent the RI and temperature sensitivities to the wavelength of a resonant peak; D is the temperature sensitivities to the Bragg wavelength.

In order to acquire the effective Bragg wavelength more accurately, a Gaussian Fitting is performed to the reflection band of the MFPI as shown in Fig. 2(a). The central wavelength is chosen as the Bragg wavelength to analyze the spectral variation. Meanwhile, the spectra are shaped through Fast Fourier Transform, spectrum filter and inverse discrete Fourier transform successively to improve the tracing accuracy of the resonant peak [24]. And then, one resonant peak is chosen and the spectrum shift is demodulated to acquire the sensitivities of temperature and RI. Consequently, the ΔRI and ΔT can be calculated through (5).

Actually, the sensing system works by tracing the Bragg wavelength and resonant peak simultaneously. It is certain that the wavelength of the resonant peak shifts along with the variation of temperature and the "advancement" of interference fringe for one full FSR would happen when temperature changes in a small range. However, not only the resonant peak but also the Bragg wavelength shifts along with the variation of temperature. For the demodulation of resonant peak shift, we take a MFPI sample as an example. Due to the Gaussian intensity modulation caused by FBGs, the resonant peaks of different orders have unique intensity characteristics. Specifically, the Bragg wavelength is firstly located by the Gaussian Fitting, and then the certain resonant peak can be easily confirmed based on the order number as shown in Fig. 2(b). Even when the temperature greatly changes from 25.6 °C to 81.2 °C, the resonant peaks shift in the same time and remain the same intensity modulation. Then, one certain peak can be located based on the order number related to the relative intensity.

The WDM technique is applied to realize quasi-distributed dual-parameter sensing. Experimentally, spectrum filtering is chosen to achieve spectrum demodulation and the environmental parametric variation can be located through the wavelength analysis. Combined with the demodulated

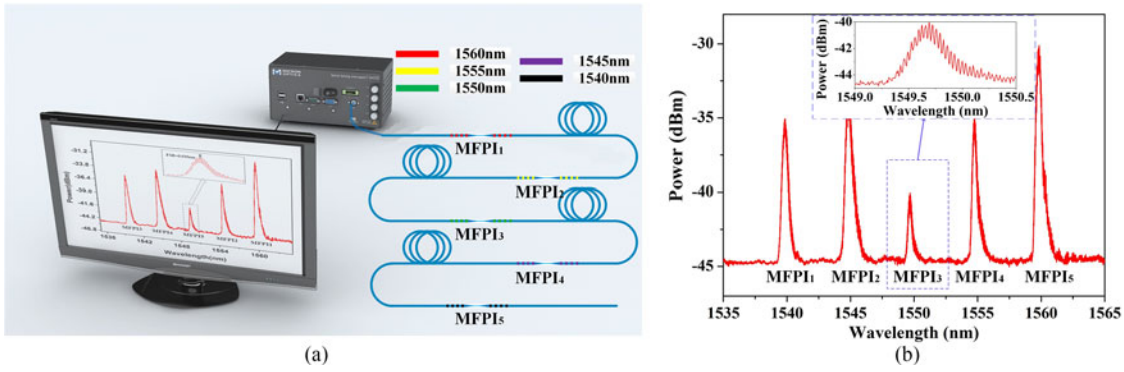

Fig. 3. (a) Configuration of the quasi-distributed RI/temperature sensing system. (b) initial spectra of the cascaded MFPIs. Inset:detailed spectrum of one sensor node.

$\Delta\lambda_R$ and $\Delta\lambda_B$, we can calculate the variation of temperature and RI based on the above sensing function.

To experimentally demonstrate the sensing performance, a prototype sensor system is constructed by 5 cascaded MFPIs with the Bragg wavelengths of 1540 nm, 1545 nm, 1550 nm, 1555 nm and 1560 nm as depicted in Fig. 3(a). All of the MFPIs are manufactured through 10-mm-long uniform FBGs with 3 dB band-width about 0.25 nm, and maximum reflectivity of 20 dB. The typical reflection spectrum is depicted in Fig. 2. Then, the central points of FBGs are bilateral-stretched to approximate 1.6 μm diameter with drawing rate of 0.15 mm/s and drawing length of 9 mm on each side. Latterly, the insertion losses of five MFPIs are measured as about 0.3 dB that means up to hundreds of sensing nodes can be multiplexed in the quasi-distributed sensing system. The reflection spectrum is obtained by the FBG interrogator (MOI SM-125) and displayed on the PC as depicted in Fig. 3(a). The initial reflective spectra of the sensing system contain five separate reflection bands and the spacings of the interference fringes are all around 0.033 nm as shown in Fig. 3(b). It should be noticed that the reflectivities of these MFPIs are some different for the reason that the heating region is not accurately the same in position and length which leads to different reflectivities of the FBGs and the diameter of the MNF is not exactly identical resulting in different transmission loss.

3. Experimental Result and Discussion

To complete the sensing functions, RI sensing experiments are carried out as follow. Subsequently, the measurement process is detailedly described in an example of $MFPI_2$. First of all, we set the MFPIs in five isolated beakers at room temperature and fill them with deionized water with RI of 1.3315. Secondly, the pure glycerinum with high refractive index is dropped in the beaker for $MFPI_2$, while the RI of solution in other beakers remains unchanged. The stabilized spectra are recorded after solution is well blended. Subsequently, the RI of glycerinum solution is measured by Abbe refractometer. Continuous ambient RI varying from 1.332 to 1.336 with step of around 0.0005 is provided and the experimental result is presented in Fig. 4. The resonant peaks of five MFPIs shift with RI varying from 1.3333 to 1.3365 are shown in Fig. 4(a) and indicate independence between the sensing units resulting from the introduced WDM technique. It is clear that the resonant peak has a distinct red shift in spectrum of $MFPI_2$ with the rise of the RI while the other sensing units are not affected neither in reflection optical power nor Bragg wavelength. Next, the above processes are repeated for other sensor units. As can be seen from Fig. 4(b), the RI sensitivities of five MFPIs are measured as 143.64 nm/RIU, 144.61 nm/RIU, 129.28 nm/RIU, 145.28 nm/RIU and 151.61 nm/RIU, respectively, and R^2 (i.e., the linearity) are 0.995, 0.996, 0.996, 0.996, and 0.997, accordingly, which demonstrates good linearity of the quasi-distributed sensing system. So it can be

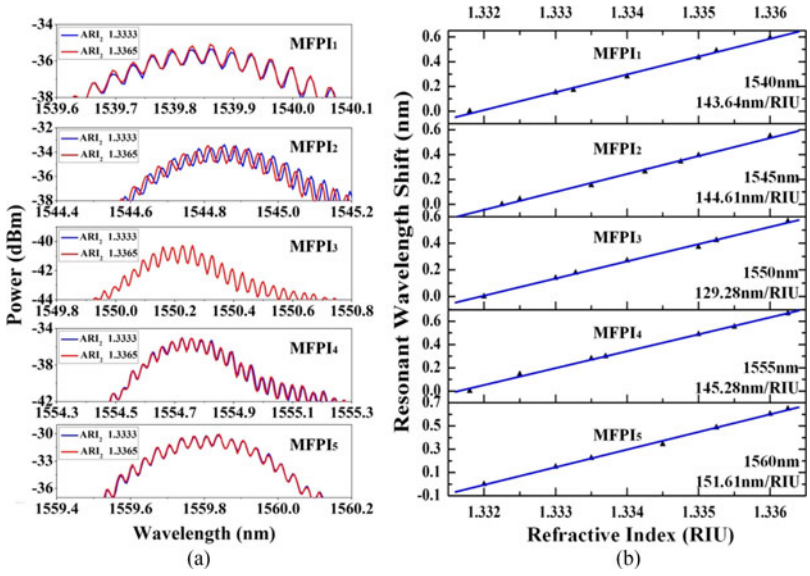

Fig. 4. (a) Detailed spectra change of MFPIs when the ambient RI around MFPI2 rises from 1.3333 to 1.3365. (b) Wavelength shift of the resonant peak as a function of ambient RI.

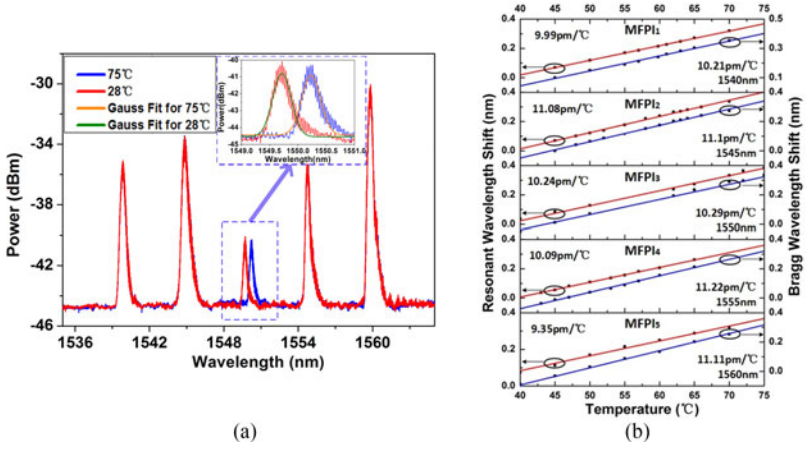

Fig. 5. (a) Reflection spectra when the environmental temperature of the MFPI3 changes from 28 °C to 75 °C. Inset: the magnified spectra of MFPI3 and Gaussian Fitting curves at 28 °C and 75 °C; (b) resonant peak wavelengths shift (red) and Bragg wavelengths shift (blue) as functions of environmental temperature.

concluded that quasi-distributed RI measurement can be realized in a long distance with our sensor system. Although the direct measurement range of RI is limited by the fringes, it can be greatly improved by the real-time wavelength tracking method [39].

Then, the temperature sensitivities experiments are carried out, separately. In detailed, the $MFPI_3$ is chosen as a representative to describe the measurement process. Experimentally, continuous external environmental temperature varying from 28 °C to 75 °C with precision of 0.1 °C is provided by a water bath, and the spectra variation is tracked and exhibited in Fig. 5(a). From the spectrum, an obvious wavelength red shift on $MFPI_3$ is observed however the others remain unchanged. And then, the Bragg wavelengths variations are acquired as shown in Fig. 5(a) (inset). In view of (1), the sensitivity of resonant peak is higher when the lower order of resonant is chosen. Thus, the 1st resonant peak of the spectra is chosen to analysis the temperature sensitivity.

Fig. 5(b) shows the demodulated Bragg wavelength variations to the temperature with the sensitivities of 10.21 pm/°C, 11.1 pm/°C, 10.29 pm/°C, 11.22 pm/°C and 11.11 pm/°C, respectively. Meanwhile, the sensitivities of 1st resonant peaks to RI are 9.99 pm/°C, 11.08 pm/°C, 10.24 pm/°C, 10.09 pm/°C and 9.35 pm/°C. Besides, the R^2 all above 0.995 are achieved which means good linearity between temperature and spectra variation (including resonant peak and Bragg wavelength). From the above, we find that temperature sensing has a good linearity and consistency.

Seen from the experimental results, there is a relative large difference in sensitivities of resonant peaks to the environmental parameters compared with Bragg wavelength which is more stable. In view of the different sensitivity, several reasons are considered to make sense. One is the diameter of microfiber is not exactly the same leading to a distinction on n_{eff} which influences the RI sensitivity. Besides, the different position and length of heating region can result in different effective length of FBG which results in a difference of the temperature sensitivity. So it can be concluded that the stability of sensitivities of the multiple MFPIs can be further improved by more precise and stable tapering technique. Further, the resonant peak tracking could be instead of the interferometric phase shifts extraction through Fast Fourier Transform technique to analysis the RI change [38], resulting in more precise demodulation.

Based on above experiment and discussion, the sensing functions of the five sensor units can be summarized as:

$$\begin{bmatrix} \Delta RI \\ \Delta T \end{bmatrix} = \begin{bmatrix} 143.64\ \text{nm}/RIU & 9.99\ \text{pm}/^{\circ}\text{C} \\ 0 & 10.21\ \text{pm}/^{\circ}\text{C} \end{bmatrix}^{-1} \begin{bmatrix} \Delta\lambda_R \\ \Delta\lambda_B \end{bmatrix} \tag{6}$$

$$\begin{bmatrix} \Delta RI \\ \Delta T \end{bmatrix} = \begin{bmatrix} 144.61\ \text{nm}/RIU & 11.08\ \text{pm}/^{\circ}\text{C} \\ 0 & 11.1\ \text{pm}/^{\circ}\text{C} \end{bmatrix}^{-1} \begin{bmatrix} \Delta\lambda_R \\ \Delta\lambda_B \end{bmatrix} \tag{7}$$

$$\begin{bmatrix} \Delta RI \\ \Delta T \end{bmatrix} = \begin{bmatrix} 129.28\ \text{nm}/RIU & 10.24\ \text{pm}/^{\circ}\text{C} \\ 0 & 10.29\ \text{pm}/^{\circ}\text{C} \end{bmatrix}^{-1} \begin{bmatrix} \Delta\lambda_R \\ \Delta\lambda_B \end{bmatrix} \tag{8}$$

$$\begin{bmatrix} \Delta RI \\ \Delta T \end{bmatrix} = \begin{bmatrix} 145.28\ \text{nm}/RIU & 10.09\ \text{pm}/^{\circ}\text{C} \\ 0 & 11.22\ \text{pm}/^{\circ}\text{C} \end{bmatrix}^{-1} \begin{bmatrix} \Delta\lambda_R \\ \Delta\lambda_B \end{bmatrix} \tag{9}$$

$$\begin{bmatrix} \Delta RI \\ \Delta T \end{bmatrix} = \begin{bmatrix} 151.61\ \text{nm}/RIU & 9.35\text{pm}/^{\circ}\text{C} \\ 0 & 11.11\text{pm}/^{\circ}\text{C} \end{bmatrix}^{-1} \begin{bmatrix} \Delta\lambda_R \\ \Delta\lambda_B \end{bmatrix} \tag{10}$$

Obviously, all the coefficient matrixes are well conditioned, and thus the sensors have relatively low error. In consideration that the WDM technique is applied to realize quasi-distributed dual-parameter sensing, the environment change can be easily positioned by the demodulation of the variation of spectra. Combined with the demodulated $\Delta\lambda_R$ and $\Delta\lambda_B$, we can calculate the variation of temperature and RI based on the above sensing function.

4. Conclusions

In conclusion, we have proposed and demonstrated a quasi-distributed fiber sensor system based on cascaded microfiber Fabry-Perot interferometers (MFPI) for simultaneous surrounding refractive index and temperature measurement. The MFPI is simply fabricated by taper-drawing a fiber Bragg grating (FBG) at its center. By demodulating the wavelength shifts of the resonant peak and Bragg wavelength with the variation of temperature and ambient RI, we can derive the sensing function with which the real-time dual-parameter sensor is realized. Moreover, wavelength-division-multiplexing (WDM) technique is applied to complete quasi-distributed sensor by using online inscribed and tapered MFPIs with different Bragg wavelengths. In this way, a quasi-distributed dual-parameter fiber sensing system is achieved and proves to be well with temperature and RI sensing. The quasi-distributed dual-parameter sensing system has great significance on monitoring gradient

parameter-variations in chemical and biological sensing applications. In practical applications, the sensing system can consist of a large number of MFPIs to monitor the RI and temperature variation in a large scale, and plastic or glass tubes are alternative to provide the MFPIs a relative stable measuring condition. We believe the system can make great progress in chemical and biological sensing, temperature and RI gradient monitor, and water pollution control.

References

[1] G. Huyang, J. Canning, M. L. Aslund, D. Stocks, T. Khoury, and M. J. Crossley, "Evaluation of optical fiber microcell reactor for use in remote acid sensing," *Opt. Lett.*, vol. 35, no. 6, pp. 817–819, Mar. 2010.

[2] L. M. Tong and M. Sumetsky, *Subwavelength and Nanometer Diameter Optical Fibers*. Hangzhou, China: Zhejiang University Press, 2009.

[3] J. S. Leng and A. Asundi, "Real-time cure monitoring of smart composite materials using extrinsic Fabry-Perot interferometer and fiber Bragg grating sensors," *Smart Mater. Struct.*, vol. 11, no. 2, pp. 249–255, Apr. 2002.

[4] M. Bravo, A. M. R. Pinto, M. Lopez-Amo, J. Kobelke, and K. Schuster, "High precision micro-displacement fiber sensor through a suspended-core Sagnac interferometer," *Opt. Lett.*, vol. 37, no. 2, pp. 202–204, Jan. 2012.

[5] Y. H. Tai and P. K. Wei, "Sensitive liquid refractive index sensors using tapered optical fiber tips," *Opt. Lett.*, vol. 35, no. 7, pp. 944–946, Apr. 2010.

[6] L. L. Xue and Y. Li, "Sensitivity enhancement of RI sensor based on SMS fiber structure with high refractive index overlay," *J. Lightw. Technol.*, vol. 30, no. 10, pp. 1463–1469, May 2012.

[7] J. H. Wo *et al.*, "Refractive index sensor using microfiber-based Mach–Zehnder interferometer," *Opt. Lett.*, vol. 37, no. 1, pp. 67–69, Jan. 2012.

[8] A. N. Starodumov, L. A. Zenteno, and D. Monzon, "Fiber Sagnac interferometer temperature sensor," *Appl. Phys. Lett.*, vol. 70, no. 1, pp. 19–21, Nov. 1997.

[9] W. H. Tsai and C. J. Lin, "A novel structure for the intrinsic Fabry-Perot fiber-optic temperature sensor," *J. Lightw. Technol.*, vol. 19, no. 5, pp. 682–686, May 2001.

[10] W. G. Jung, S. W. Kim, K. T. Kim, E. S. Kim, and S. W. Kang, "High-sensitivity temperature sensor using a side-polished single-mode fiber covered with the polymer planar waveguide," *IEEE Photon. Technol. Lett.*, vol. 13, no. 11, pp. 1209–1211, Nov. 2001.

[11] Q. Yao *et al.*, "Simultaneous measurement of refractive index and temperature based on a core-offset Mach–Zehnder interferometer combined with a fiber Bragg grating," *Sensors Actuators A, Phys.*, vol. 209, pp. 73–77, Mar. 2014.

[12] S. Gao *et al.*, "Fiber modal interferometer with embedded fiber Bragg grating for simultaneous measurements of refractive index and temperature," *Sensors Actuators B, Chem.*, vol. 188, pp. 931–936, Nov. 2013.

[13] X. Shu, B. A. L. Gwandu, Y. Liu, L. Zhang, and L. Bennion, "Sampled fiber Bragg grating for simultaneous refractive-index and temperature measurement," *Opt. Lett.*, vol. 26, no. 11, pp. 774–776, Jun. 2001.

[14] X. Liu, T. Wang, Y. Wu, Y. Gong, and Y. Rao, "Dual-parameter sensor based on tapered FBG combined with microfiber cavity," *IEEE Photon. Technol. Lett.*, vol. 26, no. 8, pp. 817–820, Feb. 2014.

[15] J. L. Li *et al.*, "Long-period fiber grating cascaded to an S fiber taper for simultaneous measurement of temperature and refractive index," *IEEE Photon. Technol. Lett.*, vol. 25, no. 9, pp. 888–891, May 2013.

[16] D. A. C. Enriquez, A. R. D. Cruz, and M. T. M. R. Giraldi, "Hybrid FBG-LPG sensor for surrounding refractive index and temperature simultaneous discrimination," *Opt. Laser Technol.*, vol. 44, no. 7, pp. 981–986, Oct. 2011.

[17] J. Shi *et al.*, "A dual-parameter sensor using a long-period grating concatenated with polarization maintaining fiber in sagnac loop," *IEEE Sensors J.*, vol. 16, no. 11, pp. 4326–4330, Mar. 2016.

[18] S. Pevec, B. Lenardic, and D. Donlagic, "Micromachining of all-fiber photonic micro-structures for microfluidic applications," *Informacije MIDEM*, vol. 46, no. 3, pp. 113–119, Oct. 2016.

[19] S. Dass and R. Jha, "Micrometer wire assisted inline Mach-Zehnder Interferometric curvature sensor," *IEEE Photon. Technol. Lett.*, vol. 28, no. 1, pp. 31–34, Jan. 2016.

[20] S. Pevec and D. Donlagic, "Miniature all-silica fiber-optic sensor for simultaneouos measurement of relative humidity and temperature," *Opt. Lett.*, vol. 40, no. 23, pp. 5646–5648, Dec. 2015.

[21] C. L. Wu *et al.*, "Low-loss and high-Q Ta_2O_5 based micro-ring resonator with inverse taper structure," *Opt. Exp.*, vol. 23, no. 20, pp. 26268–26275, Oct. 2015.

[22] P. Wang *et al.*, "Packaged optical add-drop filter based on an optical microfiber coupler and a microsphere," *IEEE Photon. Technol. Lett.*, vol. 28, no. 20, pp. 2277–2280, Jul. 2016.

[23] M. Liu *et al.*, "Dissipative rogue waves induced by long-range chaotic multi-pulse interactions in a fiber laser with a topological insulator-deposited microfiber photonic device," *Opt. Lett.*, vol. 40, no. 20, pp. 4767–4770, Oct. 2015.

[24] Z. C. Luo *et al.*, "2 GHz passively harmonic mode-locked fiber laser by a microfiber-based topological insulator saturable absorber," *Opt. Lett.*, vol. 38, no. 24, pp. 5212–5215, Dec. 2013.

[25] J. Xu *et al.*, "Self-assembled organic microfibers for nonlinear optics," *Adv. Mater.*, vol. 25, no. 14, pp. 2084–2089, Feb. 2013.

[26] H. Luo, Q. Sun, Z. Xu, D. Liu, and L. Zhang, "Simultaneous measurement of refractive index and temperature using multimode microfiber-based dual Mach–Zehnder interferometer," *Opt. Lett.*, vol. 39, no. 13, pp. 4049–4052, Jul. 2014.

[27] P. Lu, L. Men, K. Sooley, and Q. Chen, "Microstructured optical fiber for simultaneous measurement of refractive index and temperature," *Proc. SPIE*, vol. 7682, Apr. 2010, Art. no. 76820X.

[28] H. Meng, W. Shen, G. Zhang, C. Tan, and X. Huang, "Fiber Bragg grating-based fiber sensor for simultaneous measurement of refractive index and temperature," *Sensor Actuators B, Chem.*, vol. 150, pp. 226–229, Jul. 2010.

[29] C. R. Liao, Y. Wang, D. N. Wang, and M. W. Yang, "Fiber in-line Mach–Zehnder interferometer embedded in FBG for simultaneous refractive index and temperature measurement," *IEEE Photon. Technol. Lett.*, vol. 22, no. 22, pp. 1686–1688, Nov. 2010.
[30] Q. Sun, H. Luo, H. Luo, M. Lai, D. Liu, and L. Zhang, "Multimode microfiber interferometer for dualparameters sensing assisted by Fresnel reflection," *Opt. Exp.*, vol. 23, no. 10, pp. 12777–12783, May 2015.
[31] Z. Xu *et al.*, "Highly sensitive refractive index sensor based on cascaded microfiber knots with Vernier effect," *Opt. Exp.*, vol. 23, no. 5, pp. 6662–6672, Mar. 2015.
[32] H. Luo, Q. Sun, Z. Xu, W. Jia, D. Liu, and L. Zhang, "Microfiber-based inline Mach–Zehnder interferometer for dual-parameter measurement," *IEEE Photon. J.*, vol. 7, no. 2, Jan. 2015, Art. no. 7100908.
[33] J. Zhang *et al.*, "Microfiber Fabry–Perot interferometer for dual-parameter sensing," *J. Lightw. Technol.*, vol. 31, no. 10, pp. 1608–1615, May 2013.
[34] X. Li *et al.*, "Simultaneous wavelength and frequency encoded microstructure based quasi-distributed temperature sensor," *Opt. Exp.*, vol. 20, no. 11, pp. 12076–12084, May 2012.
[35] W. Ren, P. Tao, Z. Tan, Y. Liu, and S. Jian, "Theoretical and experimental investigation of the mode-spacing of fiber Bragg grating Fabry-Perot cavity," *Chin. Opt. Lett.*, vol. 7, no. 9, pp. 775–777, Sep. 2009.
[36] Y. J. Rao, "In-fibre Bragg grating sensors," *Meas. Sci. Technol.*, vol. 8, no. 4, pp. 355–375, Apr. 1999.
[37] Y. Chen, F. Xu, and Y. Lu, "Teflon-coated microfiber resonator with weak temperature dependence," *Opt. Exp.*, vol. 19, no. 23, pp. 22923–22928, Nov. 2011.
[38] J. W. Silverstone, S. McFarlane, C. P. K. Manchee, and A. Meldrum, "Ultimate resolution for refractometric sensing with whispering gallery mode microcavities," *Opt. Exp.*, vol. 20, no. 8, pp. 8284–8295, Mar. 2012.
[39] C. Gouveia *et al.*, "High resolution temperature independent refractive index measurement using differential white light interferometry," *Sensor Actuators B, Chem.*, vol. 188, pp. 1212–1217, Aug. 2013.